

# Low-Temperature Selective Catalytic Reduction of NO with NH<sub>3</sub> over Manganese Oxides Supported on Fly Ash-Palygorskite

Xianlong Zhang\*, Shuangshuang Lv, Xiaobin Jia, Xueping Wu and Fanyue Meng

School of Chemistry and Chemical Engineering, Hefei University of Technology, Hefei, 230009, PR China

## Abstract

A catalyst of manganese oxides (MnO<sub>x</sub>) supported on fly ash-palygorskite (MnO<sub>x</sub>/FA-PG) was prepared for low-temperature selective catalytic reduction (SCR) of nitric oxides (NO<sub>x</sub>) by ammonia (NH<sub>3</sub>). The influences of the preparation method, active species precursors, calcination temperature, calcination time and particle size on the SCR performance of the MnO<sub>x</sub>/FA-PG catalyst were studied. Catalysts were characterized by Brunauer-Emmett-Teller (BET) analysis, scanning electron microscopy (SEM), X-ray diffraction (XRD), X-ray fluorescent spectrometry (XRF), and NH<sub>3</sub> adsorption and temperature programmed desorption (TPD) to illustrate the physico-chemical properties of catalysts. Results showed that a negligible difference in SCR activity is observed on the MnO<sub>x</sub>/FA-PG catalyst prepared by heterogeneous deposition and wetness impregnation. Activity of the MnO<sub>x</sub>/FA-PG catalyst prepared by wetness impregnation with Mn(NO<sub>3</sub>)<sub>2</sub> as precursor was significantly superior to that of prepared with Mn(CH<sub>3</sub>COO)<sub>2</sub> as precursor. Moreover, calcination temperature significantly influenced catalytic activity. Over 70% NO conversion could be achieved at 100°C for Mn<sub>8</sub>/FA-PG catalysts calcined at 400°C for 3 h. The active component of the catalysts mainly existed in Mn<sup>4+</sup>. According to the results of NH<sub>3</sub> adsorption and temperature programmed desorption (TPD), adsorption capacity of NH<sub>3</sub> was not the decisive factor of catalytic activity and the key was the activation of adsorbed NH<sub>3</sub>.

**Keywords:** Fly ash-palygorskite; Manganese oxides; Low-temperature SCR

## Introduction

Over the past decades, nitrogen oxides from power plants and motor vehicles have been remained as major air pollutants. They can result in acid rain, photochemical smog, and ozone depletion [1,2]. Selective catalytic reduction (SCR) of NO<sub>x</sub> with NH<sub>3</sub> in the presence of oxygen is a proven technique for the removal of NO<sub>x</sub> from flue gases [3]. A large number of SCR catalysts have been explored, including noble metals [4,5], transition metal oxides [6,7] and zeolites [8,9]. Especially, V<sub>2</sub>O<sub>5</sub>-WO<sub>3</sub>/TiO<sub>2</sub> based catalysts have been extensively used in the industry [10,11]. However, the operating temperature for these catalysts is usually above 300°C, and the exhaust gases usually contain a large number of fly ash and SO<sub>2</sub>, which can easily deactivate the catalysts. Thus, the development of active SCR catalysts that can be operated at relatively low temperatures is needed.

At present, many transition metal oxides are extensively studied and proved to be highly active for low temperature SCR of NO with NH<sub>3</sub>, among which MnO<sub>x</sub>-supported catalysts attract the most concern [10,12-14]. Zhao et al. found that Mn<sub>0.06</sub>/Al<sub>2</sub>O<sub>3</sub> yields the highest NO conversion and 80% of NO conversion is obtained at 250°C and 15,000 h<sup>-1</sup> [15]. Zhang et al. reported that Mn/TiO<sub>2</sub> catalysts exhibit a high NO conversion of 90% at 100°C [16]. The high SCR activity for MnO<sub>x</sub>-supported catalysts implies that there may be an intimate connection between manganese oxides and carrier. Smirniotis et al. compared TiO<sub>2</sub>-, Al<sub>2</sub>O<sub>3</sub>- and SiO<sub>2</sub>-supported MnO<sub>x</sub> catalysts and found that the SCR performance of the supported Mn catalysts decreased in the following order: TiO<sub>2</sub> (anatase, high surface area), TiO<sub>2</sub> (rutile), TiO<sub>2</sub> (anatase, rutile), γ-Al<sub>2</sub>O<sub>3</sub>, SiO<sub>2</sub>, TiO<sub>2</sub> (anatase, low surface area) [17]. The material of carrier is directly related to the SCR activity for manganese-based catalysts.

In this paper, a solid waste material, fly ash (FA), was used as support, which can cause many problems and has become an important environmental issue [18]. Due to its moderate pore volume and pore structure, as well as its high silica and alumina contents, FA is used to prepare zeolite materials. Besides, a clay mineral, palygorskite (PG)

[19,20], was added as a binder to FA. The materials were mixed well after machine extrusion to provide an inexpensive catalyst support [21]. Manganese oxide (MnO<sub>x</sub>) was loaded as the active ingredient to produce a MnO<sub>x</sub>-supported catalyst (MnO<sub>x</sub>/FA-PG). This catalyst was then characterized through experiments in a fixed bed reactor to investigate the feasibility of using FA-PG as a catalyst support. Specific surface area [Brunauer-Emmett-Teller (BET)] analysis, scanning electron microscopy (SEM), X-ray diffraction (XRD) and X-ray fluorescent spectrometry (XRF) were used to characterise the surface properties and crystalline structures of the catalyst. NH<sub>3</sub> adsorption and temperature programmed desorption (TPD) were performed to evaluate the effect of manganese species on the surface acidity of the catalyst.

## Experimental

### Catalyst preparation

FA was obtained from the Anqing Power Plant in Anhui Province, and natural PG was acquired from Jiashan County. Main chemical composition of the molded fly ash and palygorskite are listed in Table 1. Four particle size ranges, i.e., 5-8 mm, 2-5 mm, 0.38-0.83 mm and 0.25-0.38 mm, were chosen as the experimental samples. FA-PG was pretreated at 300°C for 3 h to remove surface water. The Mn<sub>x</sub>/FA-PG catalysts were prepared firstly by heterogeneous precipitation and wetness impregnation of heat-pretreated FA-PG with Mn nitrate aqueous solution. The concentration of the solution was varied to yield

\*Corresponding author: Xianlong Zhang, School of Chemical Engineering, Hefei University of Technology, Hefei, 230009, PR China, Tel: +86-0551-6290-1450; Fax: +86-0551-6290-1450; E-mail: zhangxianlong78@126.com

Received November 25, 2015; Accepted December 02, 2015; Published December 12, 2015

Citation: Zhang XL, Lv SS, Jia XB, Wu XP, Meng FY (2015) Low-Temperature Selective Catalytic Reduction of NO with NH<sub>3</sub> over Manganese Oxides Supported on Fly Ash-Palygorskite. J Thermodyn Catal 6: 153. doi:10.4172/2157-7544.1000153

Copyright: © 2015 Zhang XL, et al. This is an open-access article distributed under the terms of the Creative Commons Attribution License, which permits unrestricted use, distribution, and reproduction in any medium, provided the original author and source are credited.

Sample	SiO <sub>2</sub>	AlO <sub>3</sub>	Fe <sub>2</sub> O <sub>3</sub>	CaO	MgO	TiO <sub>2</sub>	K <sub>2</sub> O	MnO	P <sub>2</sub> O <sub>5</sub>	SO <sub>3</sub>	FeO
FA	48.29	21.64	3.05	20.33	1.74	0.98	1.66	0.04	0.26	1.87	/
PG	69.44	11.84	5.139	0.211	12.16	0.43	0.5	0.046	0.03	/	0.08

Table 1: Main chemical composition of FA and PG (%).

different Mn loading contents. The samples were dried overnight at 110°C. Then, the specific particle sizes of catalysts were calcined in O<sub>2</sub> stream at different temperatures and times. The catalyst samples were labeled Mn<sub>x</sub>/FA-PG, MA-Mnx/FA-PG and Mn<sub>x</sub>(P)/FA-PG based on loading of the active component with different precursors and preparation methods (“x”, “MA” and “P” refer to the weight percentage of Mn loading, the Mn(CH<sub>3</sub>COO)<sub>2</sub> solution and the heterogeneous precipitation method, respectively).

### Catalyst characterization

X-ray fluorescent spectrometry (XRF) was performed on a XRF-1800 analyses (Shimadzu, Japan) to measure the chemical composition of the catalyst. X-ray Diffraction (XRD) was performed on a D/Max2500V diffractometer (Rigaku, Japan) equipped with a monochromated Cu K $\alpha$  radiation source. The catalysts were scanned at 2 $\theta$  ranging from 10°-70°. Scanning electron microscopy (SEM) images of the samples were obtained by a JSM-6490LV (Hitachi, Japan) analyser.

Brunauer-Emmett-Teller (BET) surface area was measured from the N<sub>2</sub> adsorption and desorption isotherms at -196°C using the NOVA 2200e (Quantachrome, American) adsorption analyser. Prior to analysis, 0.08-0.1 g of catalyst was preheated at 100°C for 2 h under a N<sub>2</sub> atmosphere. NH<sub>3</sub> adsorption and temperature programmed desorption (TPD) were conducted in a quartz microreactor. Then, 100 mg of the sample was preheated in Ar at 473 K for 1 h to remove any adsorbed species. Afterward, the sample was cooled to 323 K in Ar (100 mL·min<sup>-1</sup>) and 1500 ppm NH<sub>3</sub> balanced by Ar was adsorbed at this temperature with a total flow rate of 100 mL·min<sup>-1</sup> until no signal variation of NH<sub>3</sub> was detected. Subsequently, the sample was purged with 100 mL·min<sup>-1</sup> Ar until no NH<sub>3</sub> was detected in the outlet, and then ramped to 1073 K at a linear heating rate of 10 K·min<sup>-1</sup> in Ar (100 mL·min<sup>-1</sup>). The analysis of gases was performed using an online mass spectrometer QIC2000 (Hidden, Germany).

### Activity measurement

Catalyst activity was evaluated in a quartz fixed bed continuous flow reactor that operated at a pressure of 0.1 MP, and 3 g of sample was used in each test. Gas composition was 600 ppm NO, 600 ppm NH<sub>3</sub> and 3 vol% O<sub>2</sub> balanced by Ar. Total flow rate was 350 mL·min<sup>-1</sup>, which corresponds to a gas hour space velocity of 4000 h<sup>-1</sup>. NO concentrations in the inlet and outlet gases were measured online with a flue gas analyser (testo350-XL). Catalyst performance was estimated through NO conversion, which was calculated by the following equation:

$$X_{NO} = \frac{[NO]_{in} - [NO]_{out}}{[NO]_{in}} \times 100\% \quad (1)$$

Where  $[NO]_{in}$  and  $[NO]_{out}$  denote the inlet and outlet concentrations of NO, respectively.

## Results and Discussion

### Effect of different precursors and loadings on SCR activity

### over catalysts

NO conversion of Mn<sub>x</sub>/FA-PG catalyst prepared using Mn(NO<sub>3</sub>)<sub>2</sub> as a precursor is shown in Figure 1. NO conversion increased with temperature increasing at the temperature range of 100-250°C with Mn-loading. Then, it started to decrease at temperature higher than 250°C. Besides, at the same temperature, NO removal efficiency increased with increasing Mn-loading. NO conversion for Mn<sub>24</sub>/FA-PG catalyst could reach to 100% at 100°C. For FA-PG, the NO conversion was much lower in a temperature range of 100-200°C, indicating that the low temperature SCR performance of Mn-loaded catalyst was not contributed by the carrier but the MnOx itself. As shown in Figure 2, NO conversion for the MA-Mnx/FA-PG catalyst prepared using Mn(CH<sub>3</sub>COO)<sub>2</sub> as precursor was higher than that of FA-PG over the entire reaction temperature, but significantly lower than that of the Mn<sub>x</sub>/FA-PG catalyst under the same Mn-loading. It is reasonable deduced that the difference of the precursors may form different active species after calcination. Researchers also investigated the characteristics of the catalysts prepared by different precursors. However, no consensus was reached. Li et al. [22] reported that the catalyst prepared using Mn(NO<sub>3</sub>)<sub>2</sub> as precursor after calcination at 400°C mainly formed MnO<sub>2</sub> species. Meanwhile, Mn<sub>2</sub>O<sub>3</sub> species was formed when Mn(CH<sub>3</sub>COO)<sub>2</sub> was used as precursor. In addition, the catalytic activity of Mn<sub>2</sub>O<sub>3</sub> was higher than that of MnO<sub>2</sub> in the unit area. However, Wu et al. [23] considered that the catalytic activity of MnOx could be sequenced as follows: MnO<sub>2</sub>>Mn<sub>3</sub>O<sub>8</sub>>Mn<sub>2</sub>O<sub>3</sub>>Mn<sub>3</sub>O<sub>4</sub>>MnO. Further explanations about the characteristics of the catalysts prepared by different precursors will illustrate in the following.

### Effect of preparation method on SCR activity

From above results, catalysts prepared by Mn(NO<sub>3</sub>)<sub>2</sub> as precursor had high SCR activity. Thus, the NO conversion of the Mn<sub>8</sub>/FA-PG/300°C and Mn<sub>8</sub>(P)/FA-PG/300°C catalysts prepared by Mn(NO<sub>3</sub>)<sub>2</sub> as precursor at the entire reaction temperature range is shown in Figure 3. As shown in Figure 3, Mn<sub>8</sub>(P)/FA-PG catalyst had higher NO conversion than Mn<sub>8</sub>/FA-PG catalyst in the temperature range of 100-150°C. However, at the temperature higher than 200°C, NO conversion of Mn<sub>8</sub>(P)/FA-PG was lower than that of the Mn<sub>8</sub>/FA-PG catalyst. Besides, the preparation process for impregnation method was complex and led to the loss of raw materials during catalyst preparation. Based on the aforementioned results, the impregnation method is optimal and relatively economic.

### Effect of calcination temperature and calcination time on SCR activity

Based on the preceding catalyst characterization, calcination temperature and calcination time have a significant effect on the characteristics of the catalysts. In this work, we also study the effect of calcination temperature and calcination time on SCR activity. As shown in Figure 4a, the NO conversion of the Mn<sub>x</sub>/FA-PG catalyst first gradually increased, and then decreased slightly with increasing calcination temperature. When calcination temperature was 400°C, the highest SCR activity was obtained at a low temperature. In particular, over 70% NO conversion was got at 100°C and approximately 100% at 150°C. Hence, the Mn<sub>x</sub>/FA-PG catalyst that calcined at 400°C had higher SCR activity. A low calcination temperature may lead to the incomplete decomposition of Mn(NO<sub>3</sub>)<sub>2</sub> which is accompanied with NOx production during the reaction process. However, at a high calcination temperature, the structure of gesso-water and structure-water in PG might fold, which can lead to the collapse of passageways in FA-PG carriers; this condition is disadvantageous for

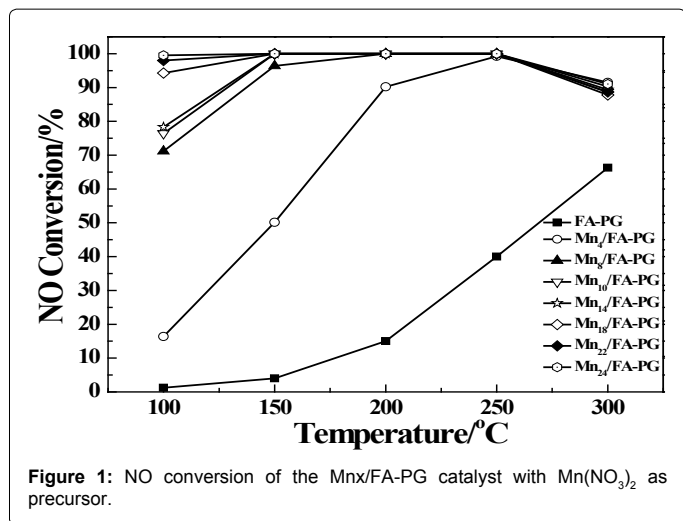


Figure 1: NO conversion of the Mn<sub>x</sub>/FA-PG catalyst with Mn(NO<sub>3</sub>)<sub>2</sub> as precursor.

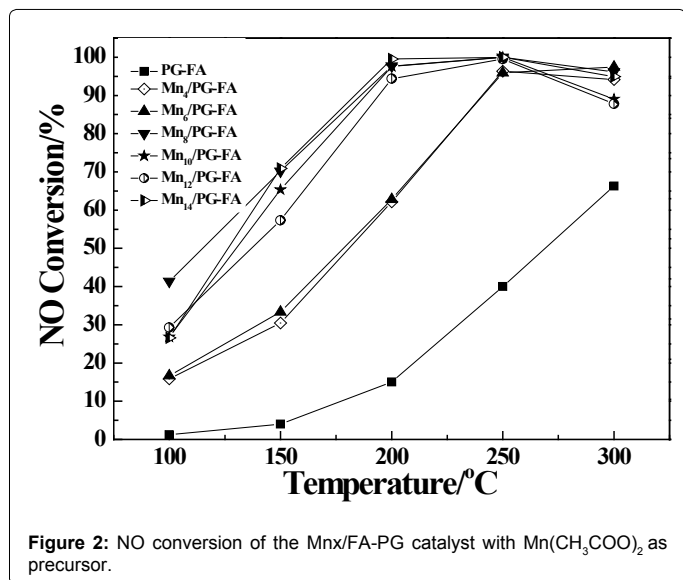


Figure 2: NO conversion of the Mn<sub>x</sub>/FA-PG catalyst with Mn(CH<sub>3</sub>COO)<sub>2</sub> as precursor.

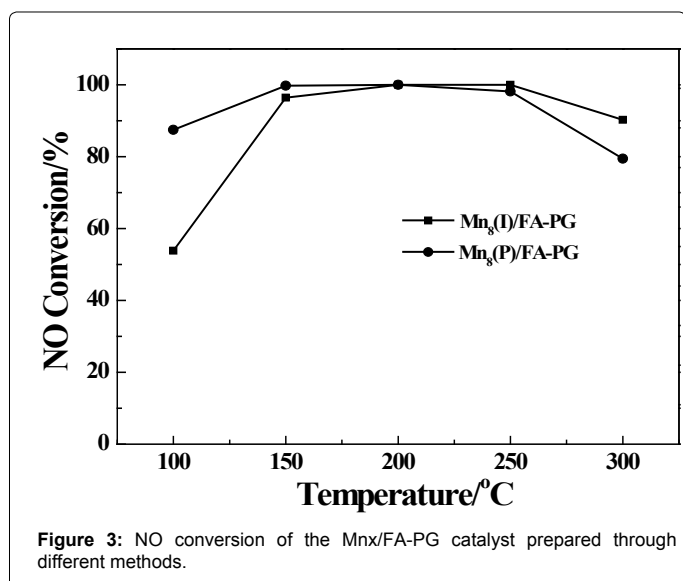


Figure 3: NO conversion of the Mn<sub>x</sub>/FA-PG catalyst prepared through different methods.

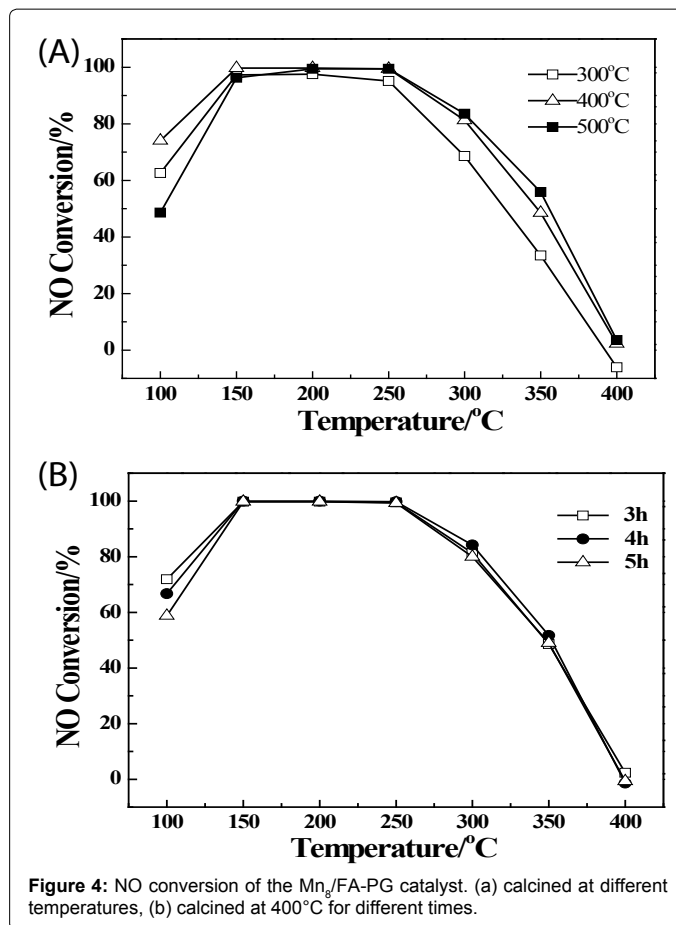


Figure 4: NO conversion of the Mn<sub>8</sub>/FA-PG catalyst. (a) calcined at different temperatures, (b) calcined at 400°C for different times.

Sample	Parameter	S <sub>BET</sub> [m <sup>2</sup> /g]
FA-PG	0.38-0.83mm	37.20
Mn <sub>8</sub> /FA-PG <sup>a</sup>	Impregnation	68.70
Mn <sub>8</sub> (P)/FA-PG <sup>b</sup>	Precipitation	72.10
Mn <sub>8</sub> /FA-PG	Mn(NO <sub>3</sub> ) <sub>2</sub>	68.70
MA-Mn <sub>8</sub> /FA-PG <sup>c</sup>	Mn(CH <sub>3</sub> COO) <sub>2</sub>	44.04
Mn <sub>8</sub> /FA-PG/300°C <sup>d</sup>	300°C	56.28
Mn <sub>8</sub> /FA-PG/400°C <sup>e</sup>	400°C	49.05
Mn <sub>8</sub> /FA-PG/500°C <sup>f</sup>	500°C	29.22
Mn <sub>8</sub> /FA-PG	4.00-8.00 mm	63.32
Mn <sub>8</sub> /FA-PG	2.00-4.00 mm	65.66
Mn <sub>8</sub> /FA-PG	0.38-0.83 mm	68.70
Mn <sub>8</sub> /FA-PG	0.25-0.38 mm	64.53

S<sub>BET</sub>: Specific surface area

Table 2: BET surface area of catalysts. (a) Mn<sub>8</sub>/FA-PG was prepared by impregnation method with Mn(NO<sub>3</sub>)<sub>2</sub> as precursor. (b) Mn<sub>8</sub>(P)/FA-PG was prepared via the heterogeneous precipitation method with Mn(NO<sub>3</sub>)<sub>2</sub> as precursor. (c) MA-Mn<sub>8</sub>/FA-PG prepared using Mn(CH<sub>3</sub>COO)<sub>2</sub> as precursor. (d) Mn<sub>8</sub>/FA-PG/300°C calcined at 300°C. (e) Mn<sub>8</sub>/FA-PG/400°C calcined at 400°C. (f) Mn<sub>8</sub>/FA-PG/500°C calcined at 500°C.

NH<sub>3</sub> adsorption [24]. The surface areas of Mn<sub>x</sub>/FA-PG catalysts under different calcination temperatures are listed in Table 2. Compared with the carrier of FA-PG, the catalysts calcined at 300°C and 400°C had large BET surface areas, but the difference between them was minimal. Meanwhile, for the catalyst calcined at 500°C, the BET surface area decreased to a certain extent. A conclusion could be drawn that an extremely high calcination temperature leads to the destruction of the support structural. Besides, the NO conversion of the Mn<sub>8</sub>/FA-PG catalyst calcined at 400°C for different times is shown in Figure 4b. As shown in Figure 4b, the NO conversion of the Mn<sub>x</sub>/FA-PG catalyst gradually decreased with increasing calcination times. Highest SCR activity was obtained when calcined at 400°C for 3 h. Thus, catalyst of Mn<sub>8</sub>/FA-PG mentioned below was all calcined at 400°C for 3 h.

### Effect of particle size on SCR activity over catalysts

Catalyst particle size has a significant effect on SCR activity. In the preparation method described above, the Mn<sub>8</sub>/FA-PG (4.00-8.00 mm), Mn<sub>8</sub>/FA-PG (2.00-4.00 mm), Mn<sub>8</sub>/FA-PG (0.38-0.83 mm) and Mn<sub>8</sub>/FA-PG (0.25-0.38 mm) catalysts were prepared to evaluate the influence of particle size on SCR activity for Mn-based catalysts. As illustrated in Figure 5, the NO conversion of the Mn<sub>8</sub>/FA-PG catalyst first gradually increased, and then decreased slightly with decreasing particle size. The Mn<sub>8</sub>/FA-PG catalyst with a particle size of 0.38-0.83 mm had a highest SCR activity, which is different from the results of Xuan [25,26]. The difference can be attributed to the material of the carrier and the preparation methods. The specific surface areas of Mn<sub>8</sub>/FA-PG catalysts under different situations are listed in Table 2. Mn<sub>8</sub>/FA-PG catalyst with a particle size of 0.38-0.83 mm had largest surface area. According to Eley-Ridal mechanism [27], the catalyst with large surface area is more conducive to the reaction gases (NH<sub>3</sub> and NO<sub>x</sub>) adsorbed on the carrier leading to the enhancement of SCR activity.

### XRD analyses

The XRD patterns of the Mn<sub>x</sub>/FA-PG catalyst prepared by wetness impregnation with Mn(NO<sub>3</sub>)<sub>2</sub> and Mn(CH<sub>3</sub>COO)<sub>2</sub> as precursors are shown in Figure 6. As shown in Figure 6a, all these patterns presented intense peaks of PG, kaolinite and dolomite due to the complex composition of FA-PG. However, there were no diffraction peaks of manganese oxides for Mn<sub>8</sub>/FA-PG and MA-Mn<sub>8</sub>/FA-PG catalysts calcined at 400°C indicating that the complex composition of FA-PG may influence the diffraction of MnOx or MnOx is uniformly dispersed on the surface of the carrier with a low percentage of active components. Thus, in this study, we particularly selected the Mn<sub>12</sub>/FA-PG and MA-Mn<sub>12</sub>/FA-PG catalysts for XRD analyses to illustrate the presence of manganese oxides. As shown in Figures 6d and 6e, the diffraction peaks of crystalline MnO<sub>2</sub> and Mn<sub>2</sub>O<sub>3</sub> phases were observed in the Mn<sub>12</sub>/FA-PG and MA-Mn<sub>12</sub>/FA-PG catalysts respectively, suggesting that MnOx in the amorphous phase is uniformly dispersed on the surface of the carrier, which is consistent with the founding by Li [22]. This finding indicated that MnOx was mainly in the form of MnO<sub>2</sub> when the Mn<sub>x</sub>/FA-PG catalyst was calcined at 400°C with Mn(NO<sub>3</sub>)<sub>2</sub> as precursor. Meanwhile, the Mn(CH<sub>3</sub>COO)<sub>2</sub> precursor mainly formed Mn<sub>2</sub>O<sub>3</sub> species. Based on the above results in Figures 1 and 2, it is reasonable deduced that catalytic activity of MnO<sub>2</sub>>Mn<sub>2</sub>O<sub>3</sub> in the unit area. The XRD patterns of the Mn<sub>12</sub>/FA-PG catalyst calcined at different temperatures are shown in Figure 7. The intensity of the diffraction peak of PG, kaolinite and dolomite for Mn-based catalyst decreased with increasing calcination temperature indicating that a high calcination temperature may destroy the primary structure of the carrier. Besides, the peaks corresponding to crystalline MnO<sub>2</sub> phase

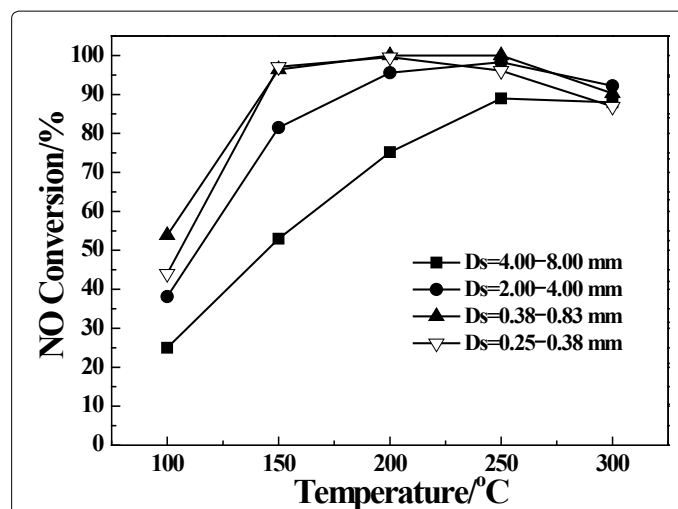


Figure 5: SCR activity of the Mn<sub>8</sub>/FA-PG catalyst with different size of particle.

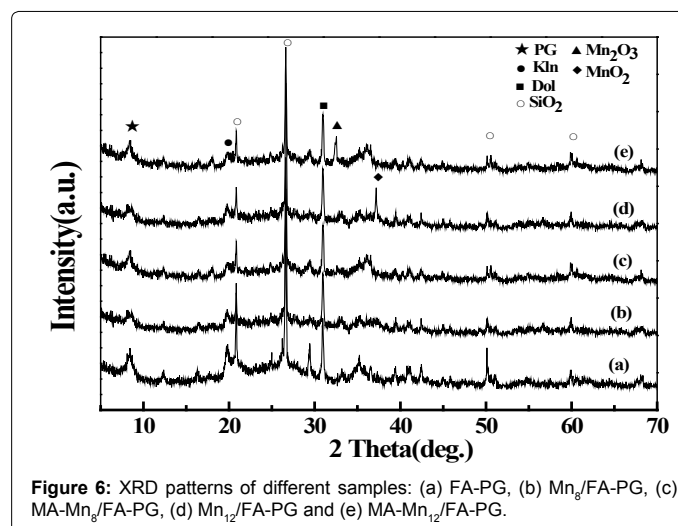


Figure 6: XRD patterns of different samples: (a) FA-PG, (b) Mn<sub>8</sub>/FA-PG, (c) MA-Mn<sub>8</sub>/FA-PG, (d) Mn<sub>12</sub>/FA-PG and (e) MA-Mn<sub>12</sub>/FA-PG.

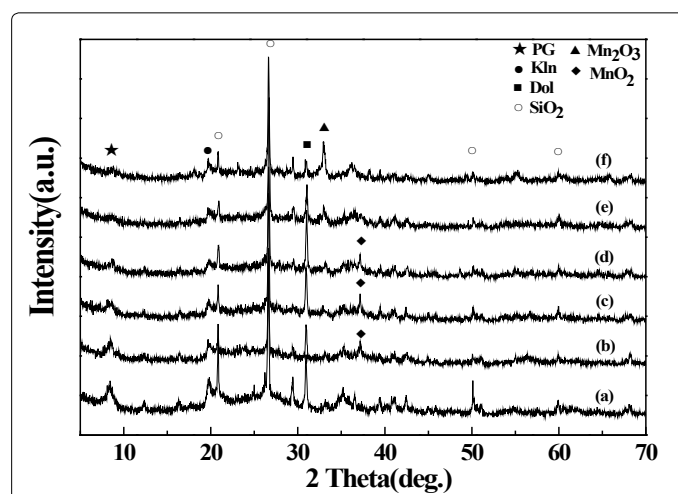


Figure 7: XRD patterns of the catalysts calcined at different temperatures: (a) Mn<sub>12</sub>/FA-PG, (b) Mn<sub>12</sub>/FA-PG/200°C, (c) Mn<sub>12</sub>/FA-PG/300°C, (d) Mn<sub>12</sub>/FA-PG/400°C, (e) Mn<sub>12</sub>/FA-PG/500°C and (f) Mn<sub>12</sub>/FA-PG/600°C.

diminished remarkably along with increasing calcination temperature and disappeared completely when calcination temperature reached over 400°C. When calcination temperature was 500°C, the diffraction peaks of Mn<sub>2</sub>O<sub>3</sub> appeared. Moreover, the diffraction peaks of Mn<sub>2</sub>O<sub>3</sub> were most prominent when calcination temperature reached to 600°C. This phenomenon is accordance with the founding by Kapteijn [28] that different calcination temperatures result in various oxidation states of manganese oxides and a high calcination temperature leads to a low valence of Mn.

### SEM of the catalysts

The electron microscopy images of the Mn<sub>x</sub>/FA-PG catalyst prepared via different methods are shown in Figure 8. These images (b-d) pertaining to the Mn<sub>8</sub>/FA-PG catalyst prepared by wetness impregnation with Mn(NO<sub>3</sub>)<sub>2</sub>, Mn(CH<sub>3</sub>COO)<sub>2</sub> as precursors and heterogeneous precipitation method, respectively. Compared to the carrier of FA-PG, there was a certain amount of white particles existed for all of the Mn-loaded catalysts, revealing that MnO<sub>x</sub> has dispersed on the surface of the catalyst after calcination. However, for Mn<sub>8</sub>/FA-PG catalyst prepared with Mn(NO<sub>3</sub>)<sub>2</sub> as precursor, the particles on the surface of the catalyst were obviously more and higher uniformly dispersed than that of MA-Mn<sub>8</sub>/FA-PG catalyst prepared with Mn(CH<sub>3</sub>COO)<sub>2</sub>, indicating that the precursor remarkably influences the morphologies of catalysts. Moreover, for MA-Mn<sub>8</sub>/FA-PG catalyst, there was a slight sintering phenomenon after being calcined, which is not conducive to improving catalyst activity. The SEM images of Mn<sub>8</sub>/FA-PG and MA-Mn<sub>8</sub>/FA-PG were agreed with the activity test in Figures 1 and 2. Besides, as shown in Figure 8d, most white globular substances (MnO<sub>x</sub>) appeared on the surface of Mn<sub>8</sub>/FA-PG catalyst prepared by heterogeneous deposition method illustrated that the catalyst exhibited the best SCR activity compared to the others [29].

### BET analyses

The physical properties of catalysts are important in determining the adsorption-desorption phenomena of gases onto its surface and influencing the activity of catalysts. Catalyst with large surface area is more conducive to the reaction gases (NH<sub>3</sub> and NO<sub>x</sub>) adsorbed on the carrier leading to the enhancement of SCR activity. Thus, the BET analyses are given and the textural properties are summarized in Table 2. Compared to the carrier of FA-PG, the surface area of catalysts increased after Mn-loaded. Mn<sub>8</sub>(P)/FA-PG prepared by heterogeneous precipitation had larger surface area than Mn<sub>8</sub>/FA-PG with impregnation. Combined with activity tests in Figure 3, it can be concluded that the larger surface area accounts for the improvement of SCR activity for Mn<sub>8</sub>(P)/FA-PG. Besides, for Mn<sub>8</sub>/FA-PG prepared with Mn(NO<sub>3</sub>)<sub>2</sub> as precursor, the BET surface area was higher than that of MA-Mn<sub>8</sub>/FA-PG prepared with Mn(CH<sub>3</sub>COO)<sub>2</sub> as precursor. Similar result was obtained for Mn<sub>8</sub>/FA-PG prepared with Mn(NO<sub>3</sub>)<sub>2</sub> as precursor. For Mn<sub>x</sub>/FA-PG catalyst with different size of particles, the catalyst with a particle size of 0.38 mm to 0.83 mm has largest surface area corresponding to the SCR activity tests in Figure 5. The specific surface areas of the Mn<sub>x</sub>/FA-PG catalyst calcined at 300°C and 400°C both exhibited a significant increase compare to the FA-PG carrier. However, the NO conversion of the Mn<sub>x</sub>/FA-PG decreased when calcined at 500°C because the carrier structure was destroyed when calcination temperature was too high.

### NH<sub>3</sub> adsorption analyses

A comparative study of NH<sub>3</sub> adsorption for the Mn(x)/FA-PG

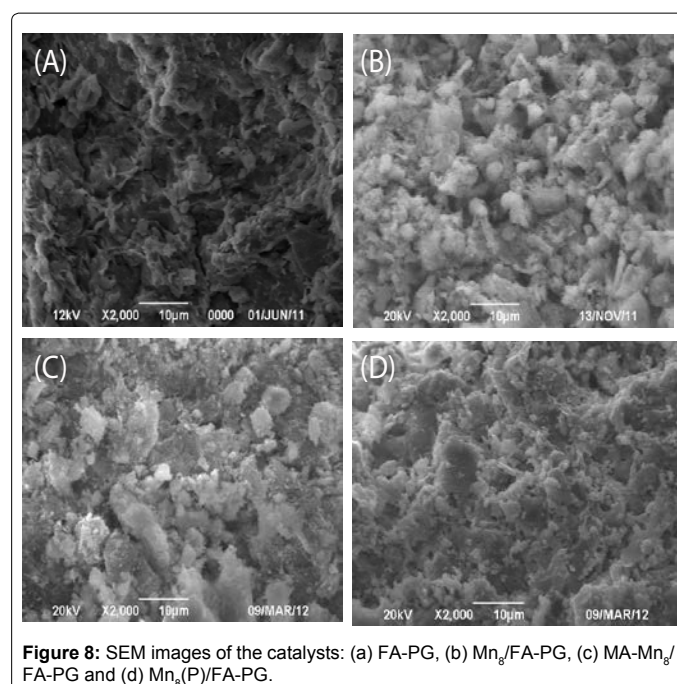


Figure 8: SEM images of the catalysts: (a) FA-PG, (b) Mn<sub>8</sub>/FA-PG, (c) MA-Mn<sub>8</sub>/FA-PG and (d) Mn<sub>8</sub>(P)/FA-PG.

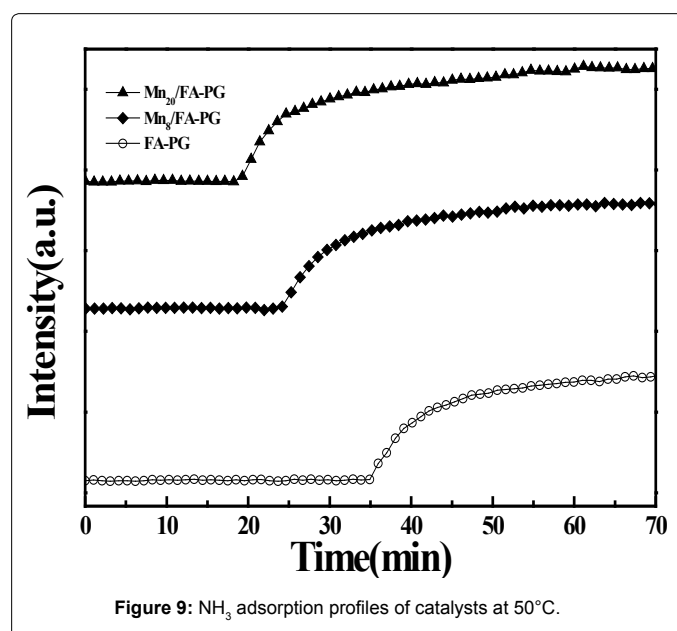


Figure 9: NH<sub>3</sub> adsorption profiles of catalysts at 50°C.

catalyst with different Mn loadings is presented in Figure 9. The penetration time of NH<sub>3</sub> was observed to decrease as Mn loading increased. This finding showed that the FA-PG carrier has a higher adsorption capacity than others. However, according to the results of BET analyses and activity test in Figure 1, the surface area of catalysts increased and the activity was improved after Mn-loaded. Thus, it can be deduced that the surface area of catalysts is not the decisive factor for NH<sub>3</sub> adsorption and the adsorption capacity of NH<sub>3</sub> not directly influence the SCR activity. Busca et al. [11] determined that the adsorption capacity of NH<sub>3</sub> influences catalytic activity. However, it was not the decisive factor and the key was the activation of adsorbed NH<sub>3</sub>.

### NH<sub>3</sub>-TPD analyses of catalysts

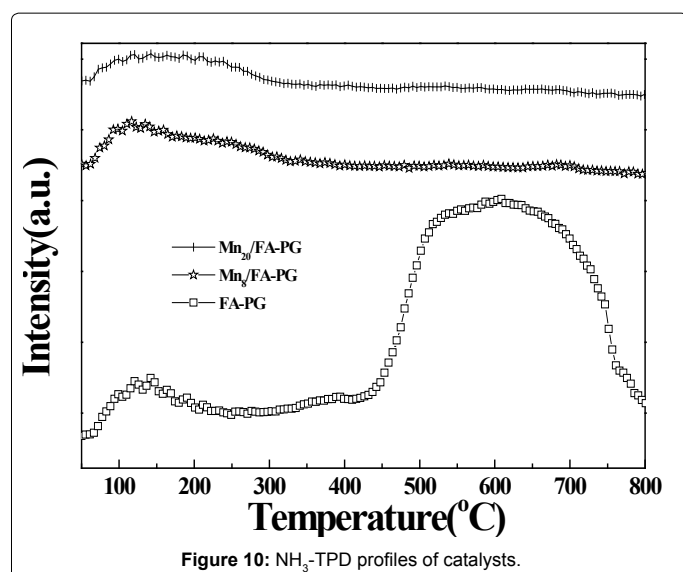


Figure 10: NH<sub>3</sub>-TPD profiles of catalysts.

NH<sub>3</sub>-TPD profiles of different Mn<sub>x</sub>/FA-PG catalysts are shown in Figure 10. Three main desorption peaks with different strength were observed at 132°C, 390°C and 603°C for FA-PG in the entire temperature range indicating that the carrier of FA-PG has three obvious acid sites. However, after manganese oxides loaded on the FA-PG, only one desorption peak at 132°C was found, and the desorption peak at 390°C and 603°C were disappeared. The peak at 132°C for Mn<sub>x</sub>/FA-PG could be assigned to the physically adsorbed of NH<sub>3</sub>. According to the founding by Greenhalgh [30], the strength of B-acid site gradually decreased with the exchange of metal ion due to the reaction between metal ions of the precursors and OH on the support surface. Therefore, the peak at 390°C and 603°C may be caused by desorption of NH<sub>3</sub> that was adsorbed on the B-acid site of the carrier itself. Besides, Busca et al. [11] indicated that, the SCR performance of Mn-based catalyst is not related to the adsorption and activation of the B-acid site, but the L-acid site.

## Conclusion

Mn<sub>x</sub>/FA-PG catalyst was highly active for SCR of NO with NH<sub>3</sub> at a temperature range of 150-300°C. Catalysts prepared by impregnation with Mn(NO<sub>3</sub>)<sub>2</sub> as precursor not only efficient but also relatively economic owing to the uniformly dispersed and high catalytic activity of MnO<sub>x</sub> on the surface of the catalyst. NO conversion closed to 100% at 100°C under Mn-loading of 24% with particle size of 0.38 μm to 0.83 μm. Moreover, catalysts calcined at 400°C for 3 h exhibited the highest activity. Most important, the SCR performance of Mn-based catalyst was not related to the adsorption and activation of the B-acid site, but the L-acid site.

## Acknowledgements

The authors gratefully acknowledge the financial support received from the National Natural Science Foundation of China (Grants Nos. 40902020, 51002042) and the Ph.D. Programmes Foundation of the Ministry of Education of China (Grant No. 20090111120019).

## References

- Zhao QS, Xiang J, Sun LS, Su S, Hu S (2009) Adsorption and Oxidation of NH<sub>3</sub> and NO over Sol-Gel-Derived CuO-CeO<sub>2</sub>-MnO<sub>x</sub>/Al<sub>2</sub>O<sub>3</sub> Catalysts. *Energy Fuel* 23: 1539-1544.
- Blanco J, Avila P, Suárez S, Yates M, Martin JA, et al. (2004) CuO/NiO monolithic catalysts for NO<sub>x</sub> removal from nitric acid plant flue gas. *Chem Eng J* 97: 1-9.
- Liu ZM, Woo SI (2006) Recent Advances in Catalytic DeNO<sub>x</sub> Science and Technology. *Catal Rev* 48: 43-89.
- Lee JH, Schmiege SJ, Oh SH (2008) Improved NO<sub>x</sub> reduction over the staged Ag/Al<sub>2</sub>O<sub>3</sub> catalyst system. *Appl Catal A: Gen* 342: 78-86.
- Itoh M, Saito M, Takehara M, Motoki K, Iwamoto J, et al. (2009) Influence of supported-metal characteristics on deNO<sub>x</sub> catalytic activity over Pt/CeO<sub>2</sub>. *J Mol Catal A: Chem* 304: 159-165.
- Shi YN, Chen S, Sun H, Shu Y, Quan X (2013) Low-temperature selective catalytic reduction of NO<sub>x</sub> with NH<sub>3</sub> over hierarchically macro-mesoporous Mn/TiO<sub>2</sub>. *Catal Commun* 42: 10-13.
- Schneider H, Maciejewski M, Kohler K, Wokaun A, Baiker A (1995) Chromia Supported on Titania: VI. Properties of Different Chromium Oxide Phases in the Catalytic Reduction of NO by NH<sub>3</sub> Studied by in Situ Diffuse Reflectance FTIR Spectroscopy. *J Catal* 157: 312-320.
- Long RQ, Yang RT (2000) Characterization of Fe-ZSM-5 Catalyst for Selective Catalytic Reduction of Nitric Oxide by Ammonia. *J Catal* 194: 80-90.
- Li J, Zhu R, Cheng Y, Lambert CK, Yang RT (2010) Mechanism of propene poisoning on Fe-ZSM-5 for selective catalytic reduction of NO(x) with ammonia. *Environ Sci Technol* 44: 1799-1805.
- Qi GS, Yang RT (2003) Low-temperature selective catalytic reduction of NO with NH<sub>3</sub> over iron and manganese oxides supported on titania. *Applied Catalysis B: Environmental* 44: 217-225.
- Busca G, Lietti L, Ramis G, Berti F (1998) Chemical and mechanistic aspects of the selective catalytic reduction of NO<sub>x</sub> by ammonia over oxide catalysts: A review. *Applied Catalysis B: Environmental* 18: 1-36.
- Kim YJ, Kwon HJ, Nam IS, Choung JW, Kil JK et al. (2010) Deactivation of Pt catalysts during wet oxidation of phenol. *Catal Today* 15: 244-250.
- Peña DA, Uphade BS, Smirniotis PG (2004) TiO<sub>2</sub>-supported metal oxide catalysts for low-temperature selective catalytic reduction of NO with NH<sub>3</sub>: I. Evaluation and characterization of first row transition metals. *J Catal* 221: 421-431.
- Zhang LF, Zhang XL, Lv SS, Wu XP, Wang PM (2015) Promoted performance of MnO<sub>x</sub>/PG catalyst for low-temperature SCR against SO<sub>2</sub> poisoning by addition of cerium oxide. *RSC Advances* 101: 82952-82959.
- Zhao W, Li C, Lu P, Wen Q, Zhao Y, et al. (2013) Iron, lanthanum and manganese oxides loaded on gamma-Al<sub>2</sub>O<sub>3</sub> for selective catalytic reduction of NO with NH<sub>3</sub> at low temperature. *Environ Technol* 34: 81-90.
- Zhang Y, Zhao X, Xu H, Shen K, Zhou C, et al. (2011) Novel ultrasonic-modified MnO<sub>x</sub>/TiO<sub>2</sub> for low-temperature selective catalytic reduction (SCR) of NO with ammonia. *J Colloid Interface Sci* 361: 212-218.
- Smirniotis PG, Srekanth PM, Peña DA, Jenkins RG (2006) Manganese oxide catalysts supported on TiO<sub>2</sub>, Al<sub>2</sub>O<sub>3</sub>, and SiO<sub>2</sub>: A comparison for low-temperature SCR of NO with NH<sub>3</sub>. *Industrial & Engineering Chemistry Research* 45: 6436-6443.
- Rubel A, Andrew R, Gonzalez R, Groppo J, Robl T et al. (2005) Adsorption of Hg and NO<sub>x</sub> on coal by-products. *Fuel* 84: 911-916.
- Chen TH, Xu XC (2004) Nanometer Mineralogy and Geochemistry of palygorskite clays in the Border of Tiangsu and Anhui provinces. Beijing: Science press.
- Zhang XL, Lv SS, Zhang CP, Wu XP, Zhang LF, et al. (2015) Effect of SO<sub>2</sub> on SCR activity of MnO<sub>x</sub>/PG catalysts at low temperature. *Chemical Papers* 69: 1548-1555.
- Sun XG, Yun D, Zhang P, Guo LY, Yao Q (2010) De-NO<sub>x</sub> Performance of Modified Fly Ash Supporting SCR Catalyst Under Various Molding Techniques. *Journal of Combustion Science and Technology* 2: 133-136.
- Li JH, Chen JJ, Ke R, Luo CK, Hao JM (2007) Effects of precursors on the surface Mn species and the activities for NO reduction over MnO<sub>x</sub>/TiO<sub>2</sub> catalysts. *Catal Commun* 8: 1896-1900.
- Wu BJ, Liu XQ, Wang SG, Zhu L, Cao LY (2008) Investigation and characterization on MnO<sub>x</sub>/TiO<sub>2</sub> for low-temperature selected catalytic reduction of NO<sub>x</sub> with NH<sub>3</sub>. *Journal of Combustion Science and Technology* 14: 221-226.
- Chen TH, Wang J, Qing CS, Peng SC, Song YX (2006) Effect of heat treatment on the Palygorskite structure morphology, and surface properties. *Ceramic Society* 34: 1406-1410.

- 
25. Xuan XP, Yue CT, Yao Q, Li SY (2003) Selective catalytic reduction of NO by ammonia with fly ash catalyst. *Energy & Fuel* 82: 575-579.
  26. Xuan XP, Yue CT (2003) The selective catalytic reduction of NO by ammonia with fly ash catalyst. *Journal of Environmental Science* 23: 33-38.
  27. Marban G, Valdes-Solis T (2004) Mechanism of low-temperature selective catalytic reduction of NO with NH<sub>3</sub> over carbon-supported Mn<sub>3</sub>O<sub>4</sub> Role of surface NH<sub>3</sub> species: SCR mechanism. *Journal of catalysis* 226: 138-155.
  28. Kapteijn F, Smgoredjo L, Andreml A (1994) Activity and selectivity of pure manganese oxides in the selective catalytic reduction of nitric oxide with ammonia [J]. *Applied Catalysis B: Environmental* 3: 173-189.
  29. Jiang B, Liu Y, Wu Z (2009) Low-temperature selective catalytic reduction of NO on MnO(x)/TiO(2) prepared by different methods. *J Hazard Mater* 162: 1249-1254.
  30. Greehalgh B, Fee M, Dobri A, Moir J, Burich R (2010) DeNO<sub>x</sub> activity-TPD correlations of NH<sub>3</sub>-SCR catalysts. *Journal of Molecular Catalysis A: Chemical* 333: 121-127.